Proceedings of the XVII ECSMGE-2019
Geotechnical Engineering foundation of the future
ISBN 978-9935-9436-1-3

doi: 10.32075/17ECSMGE-2019-0516

XVII European Conference
ECSMGE 2019
Reykjavík
on Soil Mechanics
and Geotechnical Engineering

Effects of geosynthetic inclusions on the fatigue and fracture properties of asphalt overlays

Effets des inclusions géosynthétiques sur les propriétés de fatigue et de rupture des couches de revêtement en asphalte

J. Polidora
Florida Department of Transportation, Boca Raton, United States

K. Sobhan and D.V. Reddy
Florida Atlantic University, Boca Raton, United States

ABSTRACT: Flexible or asphalt pavements constitute nearly 94% of the 2.7 million miles of existing roadways in the United States. In a typical rehabilitation project, the existing asphalt pavement is milled up to a prescribed depth for removing the near surface distresses such as excessive cracking and rutting, and a new overlay is placed. The average time between resurfacing projects varies depending on the level of pavement deterioration which is significantly accelerated when poor subgrade conditions are encountered. The use of geosynthetic reinforcement within the new asphalt overlay is often perceived as a mitigation strategy that can delay the onset and propagation of reflection cracking, and control pavement rutting. However, some mixed reviews about the performance of the geosynthetic reinforced overlays have been reported in the literature. A laboratory investigation was conducted for evaluating the flexural fatigue behavior, permanent deformation response, and fracture characteristics of geogrid reinforced asphalt beam specimens made from a typical overlay material. The laboratory specimens included geogrid as a single-layer inclusion either at the bottom third depth or at the mid height, and as double-layer inclusion, with geogrid placed both at the bottom third and at the middle of the beam. It was found that the geogrid reinforcement, when used in double layers, can substantially improve the fatigue and fracture properties of asphalt beams compared to unreinforced specimens. It is therefore concluded that geogrid reinforcement can potentially extend the service life of asphalt overlays for long term preservation of the pavement system.

RÉSUMÉ: Les chaussées souples ou asphaltées représentent près de 94% des 2,7 millions de milles de routes existantes aux États-Unis. Dans le cadre d'un projet de remise en état typique, la chaussée asphaltée existante est fraisée jusqu'à une profondeur prescrite pour éliminer les affaissements superficiels, comme les fissures et les ornières excessives, et une nouvelle couche est placée. Le temps moyen entre les projets de resurfaçage varie selon le niveau de détérioration de la chaussée qui s'accélère considérablement lorsque de mauvaises conditions de fondation sont rencontrées. L'utilisation d'un renforcement géosynthétique dans le nouveau revêtement d'asphalte est souvent perçue comme une stratégie d'atténuation qui peut retarder le début et la propagation de la fissuration par réflexion et contrôler l'ornière de la chaussée. Toutefois, la documentation fait état de certaines critiques partagées au sujet de la performance des recouvrements renforcés géosynthétiques. Une étude en laboratoire a été menée pour évaluer le comportement en fatigue flexurale, la réponse à la déformation permanente et les caractéristiques de rupture d'échantillons de poutres d'asphalte renforcées par des géogrilles, fabriqués à partir d'un matériau de recouvrement typique. Les spécimens de laboratoire incluaient des géogrilles en une seule couche, soit à la profondeur du tiers inférieur ou à la hauteur moyenne, et en une double couche, avec des géogrilles placées à la fois au tiers inférieur et au milieu du faisceau. Il a été constaté que l'armature

géogridée, lorsqu'elle est utilisée en couches doubles, peut améliorer considérablement les propriétés de fatigue et de rupture des poutres en asphalte par rapport aux échantillons non renforcés. On conclut donc que l'armature géogridée peut potentiellement prolonger la durée de vie des recouvrements d'asphalte pour la préservation à long terme du système de chaussées.

Keywords: Asphalt Overlays, Geosynthetic Inclusions, Fatigue, Fracture

1 INTRODUCTION

Out of nearly 2.7 million miles (4.3 million kilometers) of paved roads in the U.S., 94% is asphalt (flexible) pavements (NAPA, 2017). In most resurfacing or rehabilitation project, the existing asphalt pavement is milled and an overlay is placed. The average time between resurfacing projects varies depending on the level of pavement deterioration which is significantly accelerated when soft soils and poor subgrade conditions are encountered. Use of geosynthetics in the overlay may provide an effective near surface strategy to mitigate premature deterioration. However, some mixed reviews about the performance of the geosynthetic overlay have been found in the literature (Bush and Brooks, 2007).

Motivation for the current study stems from the experience gathered during the construction and monitoring of 24 experimental test sections along the SR 15 / US 98 roadway in southeastern Florida (Sobhan and George, 2011; Sobhan et al. 2010), out of which 8 were control sections, and 16 sections were reinforced with various geosynthetics and steel reinforcing products embedded in the new asphalt overlays. Deep deposits of organic soils and peats at shallow depths in this region are known to cause premature pavement distresses requiring frequesnt and costly rehabilitation. Long-term monitoring data on the experimental sections continued to show relatively better performance by the reinforced overlays compared to the control sections in terms of cracking and rutting. To have a better understanding of the effectiveness of geosynthetics within the overlay, the current laboratory investigation was undertaken to specifically evaluate the fatigue, fracture and permanent deformation behavior of a geosynthetic reinforced asphalt overlay material. These mechanical characteristics are generally linked to the cracking and rutting behavior of flexible pavement overlay in the field. In addition, the efforts are made to determine the optimum location and effects of multilayer geosynthetics within the overlay system for maximizing performance.

2 RESEARCH OBJECTIVES

Based on foregoing discussions, the current objectives of this research are:

1. To determine the benefits of including geosynthetic reinforcement on the fatigue life of a model asphalt overlay;
2. To determine the benefits of including geosynthetic reinforcement on the fracture properties of an asphalt overlay;
3. To characterize the permanent deformation accumulation process in reinforced asphalt overlay due to cyclic loading;
4. To determine the optimum location and/or the number of reinforcing layers for enhanced performance of the overlay.

3 MATERIALS USED

Asphalt concrete used in this study was donated by Ranger Construction located in West Palm Beach Florida. Materials were obtained at the plant and transported back to Florida Atlantic University for laboratory compaction and testing.

The geosynthetic material used in this study was GlasGrid 8501 manufactured by Tensar Corporation.

4 EXPERIMENTAL PROGRAM

The mix design used for the asphalt beams were based on Florida Department of Transportation (FDOT) specification for hot in-place recycled mix. FDOT has standard specifications for all products and materials used in roadway construction. Section 334, Superpave Asphalt Concrete, provides guidance including the production range for asphalt binder content, percent passing No. 200 sieve, etc (2009). Pavement recycling involves heating the asphalt, milling it, adding aggregates, mixing it, and then placing it on the prepared subgrade (Ali and Sobhan, 2011). A mold was fabricated at FAU to pour and roller-compact the Superpave quality asphalt to produce 21" long x 3.75" thick x 4" wide beams (533 mm x 95 mm x 102 mm). A total of 45 beams were prepared out of which 15 were unreinforced and 30 were reinforced. Beam were stored at room temperature for at least 24 hours. The geosynthetics were either placed at the middle, or at bottom third depth of the specimen. Several beams were double reinforced with one layer placed at the bottom-third depth, and another layer at the middle. The geosynthetics locations are shown in Figure 1. Due to the anticipated variability in fatigue experiments, a sufficient number of specimens needed to be tested to produce the so-called S-N (stress ratio, S, versus cycles to failure, N) curve.

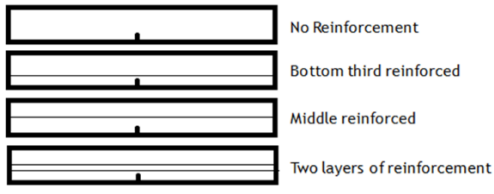

Figure 1. Location of Geosynthetic Reinforcements

A total of 30 single-edge notched beams, SENB, were prepared for fracture testing. These beams contain a small notch (6.35 mm) to create a stress concentration and induce failure by crack propagation. There are two options for preparation of notched specimens. The first option is cutting a notch directly into the compacted and cured beam. This method may result in a blunt notch tip. To avoid this, a two-step method was adopted. First, a wet masonry saw was used to cut the notch to half of its depth. Next, the final depth was reached by using a handsaw with a metal cutting blade.

Static testing (using monotonically increasing load) was conducted first on notched and un-notched specimens to determine the modulus and fracture properties of the material. The P-Δ curve was developed based on static testing, loading the beams to failure. All beams in this study had 15% RAP content, with 15% being the current industry standard. A total of 24 beams were subjected to static testing.

A total of 18 notched specimens were used for fatigue testing. The fatigue testing was conducted approximately in accordance with ASTM D7460-10 (2010) under a four-point bending configuration. All tests were conducted under load control at a frequency of 2 Hz, similar to Ling and Liu (2001), with loading amplitude based on the results of the static testing. This study displayed an increase in stiffness and bearing capacity of the asphalt concrete pavement.

5 RESULTS OF STATIC TESTING

Under static loading, three of each type of beam were tested in flexure. Figure 2 shows the load-deflection or P-Δ curves for four types of unnotched beams: unreinforced (SUU), middle reinforced (SMU), bottom-third reinforced (SBU), and double reinforced (SDU). It is found that the reinforced beams in general were able to withstand higher loads, and showed higher ductility compared to unreinforced beams, with

the double reinforced beams showing the highest capacity.

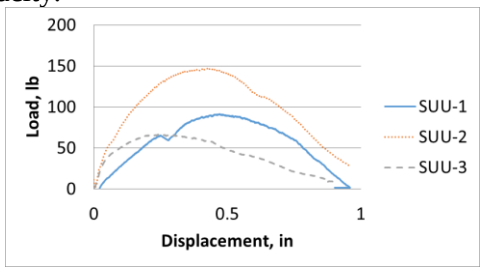

(a)

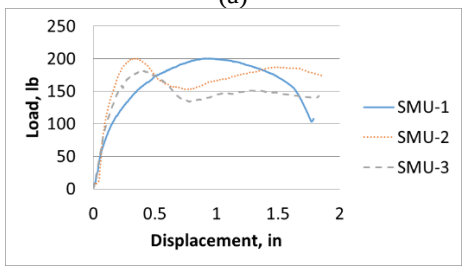

(b)

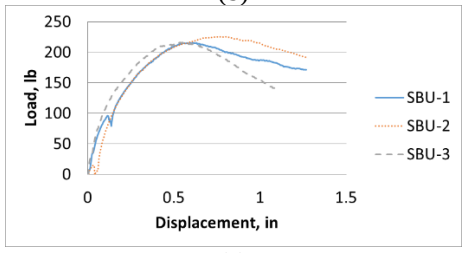

(c)

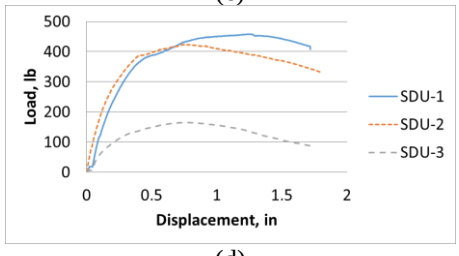

(d)

Figure 2. P-Δ curves for (a) Unreinforced, (b) Middle Reinforced, (c) Bottom-Third Reinforced and (d) Double Reinforced

Figure 3 shows the location and mode of crack propagation in various beams moments before failure. At failure, the cracks in the unreinforced beams propagated all the way to the top of the beams creating a total catastrophic failure of the specimen.

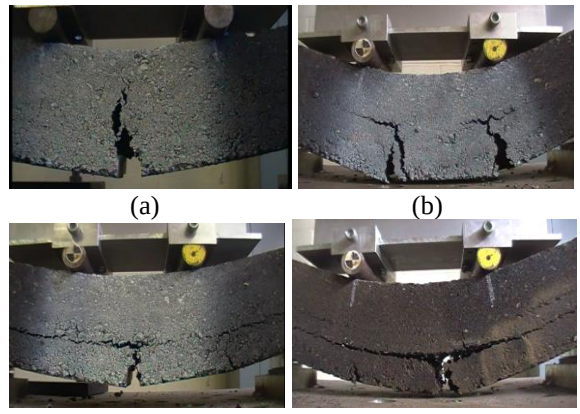

(a) (b)

(c) (d)

Figure 3. Crack Propagation in Static Testing: (a) Unreinforced, (b) Middle Reinforced, (c) Bottom-Third Reinforced and (d) Double Reinforced

On the other hand, in the reinforced beams, the geosynthetics deflected the propagating crack along the reinforcing layer, allowing the beam to withstand higher loads for a longer period of time.

6 RESULTS OF FATIGUE TEST

Fatigue testing was conducted to determine the relationship between stress ratio (SR) and the number of cycles to failure (N) or the so-called SR-N curve, the fatigue life, and the crack propagation rate of notched specimens. Based on the results of the static tests, fatigue tests were only conducted on the remaining beam type: unreinforced, bottom third reinforced and doubly reinforced.

6.1 Analysis of Fatigue Test Results

All fatigue tests were conducted approximately in accordance with AASHTO T321 procedures. Each type of beam went through a testing regimen of five beams at various stress ratios. Due to variabilities in the strengths of individual beams of the same type and mix design, it is always a challenge to estimate the *exact* stress ratio, which is the ratio of the applied stress to the actual flexural strength of the tested beam. In order to have a better estimate of the stress ratio,

two different approaches were followed. Approach 1 involved using a broken half from the tested unreinforced beams and loading the half beams to failure in 3-point bending. This provided the flexural strengths of the beams. The average flexural strengths thus obtained was used to calculate the stress ratio for that particular beam.

In Approach 2, one full size, notched beam of each type was tested to failure to obtain the flexural strength. and to use these values for the calculation. Additionally, since these beams are notched, the stress concentration factor, *K*, was applied to determine the appropriate flexural strength as per Hibbler (2005). Details of this procedure are available elsewhere (Polidora, 2017).

Figure 4 shows the SR-N curves for various types of beams using the two approaches outlined above to calculate stress ratios. It is found that the bottom-third and double reinforced beams were able to withstand substantially more number of cycles to failure compared to unreinforced beams. The relationship between SR and N can be expressed as:

$$SR = c + Alog(N) \qquad (1)$$

where c and A are material parameters. These relationships are shown in Table 1.

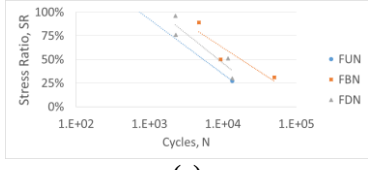

(a)

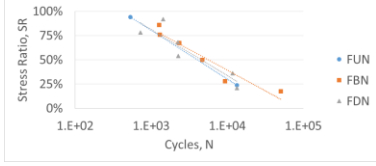

(b)

Figure 4: Stress Ratio vs. Number of Cycles to Failure for Fatigue Tests on Notched Beams (a) Approach 1 and (b) Approach 2

Table 1. Empirical Models for SR-N Curves

	Beam Type	Equation
Approach 1	Unreinforced	SR = 2.73-0.6237log(N)
	Bottom-Third	SR = 2.65-0.5082log(N)
	Double	SR = 2.95-0.6273log(N)
Approach 2	Unreinforced	SR = 2.38-0.5428log(N)
	Bottom-Third	SR = 2.10-0.4297log(N)
	Double	SR = 2.24-0.4759log(N)

6.2 Permanent Deformation Analysis

At each cycle of loading and unloading, there is a recoverable deformation, ΔR and a permanent deformation, ΔP such that

$$\Delta T = \Delta P + \Delta R \qquad (2)$$

where ΔT equals the total deformation. This is schematically shown in Figure 5.

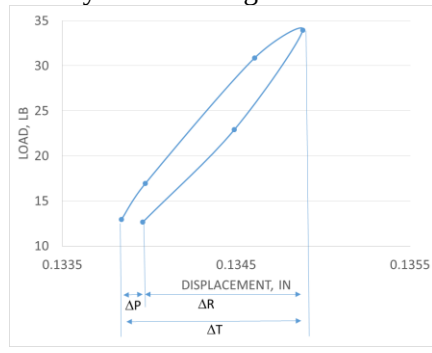

Figure 5. Permanent Deformation for each Cycle in a typical Fatigue Testing (FUN-1)

The permanent deformation at each cycle is calculated from the measured deformation. Figure 6 shows the variation of accumulated permanent deformation (normalized by the maximum permanent deformation, ΔP_{max}, with the number of loading cycles, N_i (normalized by the number of cycles to failure, N_f). The average

values for ΔP_{max} were 0.68 in. for the unreinforced beams, and 0.75 in. for the reinforced beams, respectively.

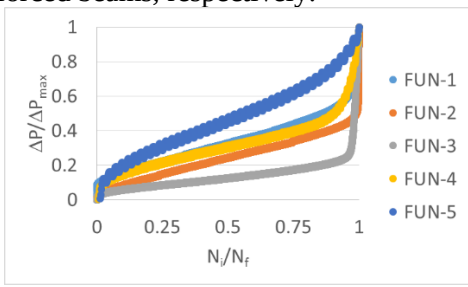

(a)

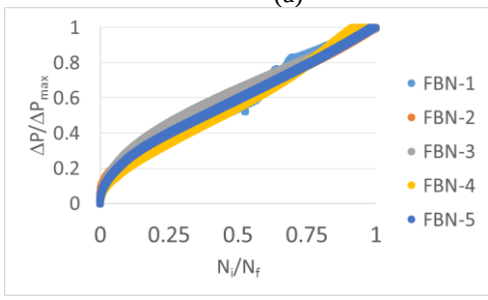

(b)

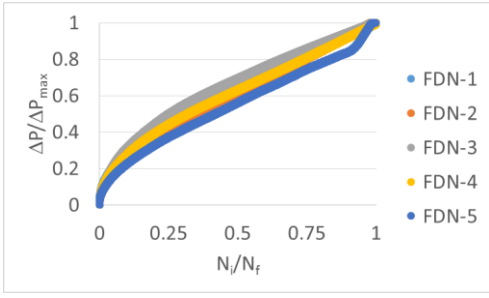

(c)

Figure 6. Accumulated Deformation for (a) Unreinforced, (b) Bottom-Third Reinforced and (c) Double Reinforced Beams

It is observed from Figure 6 that the accumulation of permanent deformation in unreinforced specimens, in general, consist of three phases: (i) A rapid growth phase, typically up to about 10% of the fatigue life; (ii) A stabilized phase, typically ranging from 10% to 90% of the fatigue life; and (iii) A catastrophic failure phase, typically ranging between 90% to 100% of the fatigue life. For reinforced specimens, a rapid growth phase (up to 10%) is followed by a gradually increasing phase up to failure, but the catastrophic phase appears to be nonexistent. This indicates that the reinforced overlay will exhibit a prolonged occurrence of rutting induced failure.

7 FRACTURE CRACK GROWTH RATE

The fracture crack growth rate was measured and analyzed for each beam to determine how the addition of the geosynthetics affects the crack propagation rate based on Paris' Law given by Equation 3 (Anderson, 2005).

$$\frac{d_a}{d_n} = k_1\left(\Delta K^{k_2}\right) \qquad (3)$$

where a is the crack (notch) size, N is the number of cycles, ΔK is the stress intensity factor, and the average values of k_1 and k_2 are found in Table 2.

Table 2: Experimentally Obtained Values of k_1 and k_2

	k_1	k_2
FUN	9.77	2.11
FBN	0.010	1.14
FDN	0.011	1.11

The crack growth was measured using video imaging techniques described elsewhere (Polidora, 2017). The crack growth rate, da/dN was determined for each beam and correlated with the change in the stress intensity factor, ΔK (Figure 7). The following empirical crack growth rate models are proposed for the unreinforced, bottom-third and double reinforced beams:

Unreinforced Beam:

$$\frac{d_a}{d_N} = 9.77(\Delta K)^{2.11} \qquad (4)$$

Bottom-Third Reinforced Beam:

$$\frac{d_a}{d_N} = 0.10(\Delta K)^{1.14} \qquad (5)$$

Double Reinforced Beam:

$$\frac{d_a}{d_N} = 0.011(\Delta K)^{1.11} \qquad (6)$$

Results indicate that the reinforced beams demonstrate lower fatigue crack growth rate compared to unreinforced specimens.

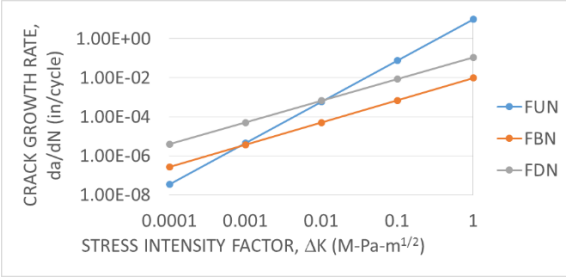

Figure 7: Paris' Law for Unreinforced, Bottom-Third Reinforced and Double Reinforced Beams

8 CONCLUSIONS

The specific conclusions drawn from the study are as follows:

1. Benefits of geosynthetic inclusions: The geosynthetic reinforcement significantly improved the static load carrying capacity of asphalt beams as compared to unreinforced beams. During fatigue testing, the reinforced specimens demonstrated higher fatigue resistance (SR-N curves), and considerably lower fatigue crack growth rate (according to Paris's Law), in comarison with unreinforced specimens.
2. Permanent deformation response: For all specimens, the permanent deformation accumulated gradually with the loading cycles. However, beyond 90% of the fatigue life, the unreinforced specimens suffered a catastrophic increase in the accumulation of permanent deformation leading to failure, while the reinforced specimens continued to deform at a gradual rate until failure representing a more ductile behavior and prolonged failure.
3. Location of reinforcement: The double reinforced beams performed best in terms of strength properties during static testing. During cyclic testing, there was minimal difference in fatigue resistance between the reinforced beams (bottom-third or double reinforced) based on the SR–N relationships. However, the double reinforced beams demonstrated the slowest crack growth rate based on Paris's Law. Accordingly, incorporating double layers of a suitable geosynthetic reinforcement in the asphalt overlay may be beneficial for long term performance, and should be considered in design.

9 ACKNOWLEDGEMENTS

We would like to acknowledge the FAU Civil, Environmental and Geomatics Engineering Department for use of the geotechnical and material laboratories.

10 REFERENCES

Ali, H., and Sobhan, K. (2012). "On the Road to Sustainability: Properties of Hot in-place Superpave Mix," Transportation Research Record, Journal of the Transportation Research Board, Volume 2292, pp. 88-93.

Anderson, T. (2005). *Fracture Mechanics*. Boca Raton: CRC Press, 3E.

ASTM. (2010). ASTM D 7460: Standard Test Method for Determining Fatigue Failure of Compacted Asphalt Concrete Subjected to Repeated Flexural Bending. West Conshohocken: ASTM International.

Bush, A. J., & Brooks, E. W. (July 2007). Geosynthetic Materials in Reflective Crack Prevention. Salem: Oregon Department of Transporation.

FDOT. (2009). Superpave Hot Mix Asphalt. FDOT Specifications.

Ling, H. I., & Liu, Z. (2001). Performance of Geosynthetic-Reinforced Asphalt Pavement.

Journal of Geotechnical and Geoenvironmental Engineering, Volume 127, Issue 2. 177-184.

National Aapahlt Pavement Association (NAPA) (2017). Engineering Overview. Lanham, MD. www.asphaltpavement.org.

Polidora, J. (2017). *Fracture and Fatigue Behavior of Geosyntheic Reinforced Asphalt Concrete For Pavement Overlays*, PhD Dissertation, Florida Atlantic University, Boca Raton, FL.

Sobhan, K. and George, K. P. (2011). Surface Pavement Solutions for Poor Subgrade Conditions Phase II: Performance Analysis of Test Sections and Implementation Guidelines, Final Report, Florida Department of Transportation.

Sobhan, K., George, K. P., Pohly, D. and Ali, H. (2010). "Stiffness Characterization of Reinforced Asphalt Pavement Structures Built Over Soft Organic Soils," Transportation Research Record: Journal of the Transportation Research Board, Volume 2186, pp. 67-77.